Proceedings of the 11th International Symposium on
Computer Applications in Biotechnology (CAB 2010),
Leuven, Belgium, July 7-9, 2010
Julio R. Banga, Philippe Bogaerts, Jan Van Impe,
Denis Dochain, Ilse Smets (Eds.)

The Estimation of Stability Boundaries for an Anaerobic Digestion System

Mihaela Sbarciog * **Mia Loccufier** * **Erik Noldus** *

* *Department of Electrical Energy, Systems and Automation, Ghent University, Technologiepark 914, B-9052 Zwijnaarde, Belgium (e-mail: mihaela@ autoctrl.UGent.be, mia.loccufier@ UGent.be, noldus@ autoctrl.UGent.be).*

Abstract: The operation of biochemical reaction systems requires substantial expertise and a good understanding of system dynamics. Due to various inhibition effects, these systems usually possess several equilibrium points. Selecting the initial state of the system is as important as selecting the system's inputs for a proper operation and for achieving the technological goal. This paper presents an anaerobic digestion system with two biochemical reactions, which possesses six equilibria for some ranges of system's inputs. The system's stability boundary separates the set of initial states from which the system converges to the desired operating point and the set of initial states which lead the system to a totally undesired condition, the acidification point. A methodology for estimating this stability boundary is described. Additionally, a procedure for visualizing the extent of the estimated boundary in a lower dimensional space is introduced. The algorithms are simple and provide accurate estimates. Moreover, the results may be displayed as two-dimensional diagrams that can be easily understood by the system's operator.

Keywords: nonlinear systems, system analysis, stability domain, anaerobic digestion, biotechnology

1. INTRODUCTION

The term anaerobic digestion refers to a series of multi-substrate multi-organism biological processes that take place in the absence of oxygen and by which organic matter is decomposed and converted to biogas (see Alcaraz-González et al. (2005)).

Anaerobic digestion provides several advantages: a high capacity to treat slowly degradable substrates (plant residues, animal wastes, wastewater, etc.) at high concentrations, a low sludge production, the possibility to produce valuable intermediate metabolites, low energy requirements and the possibility for energy recovery through methane combustion. However, in spite of these advantages, anaerobic treatment plants are seldom used at industrial scale (Mailleret et al. (2003)). Substantial expertise is required to operate such systems because they are known to become easily unstable: an accumulation of intermediate compounds can lead to the crash of the digester.

To avoid this problem several control strategies have been proposed in literature (Perrier and Dochain (1993), Mailleret et al. (2003), Mailleret et al. (2004)), which ensure either the local or the global stability of the process. However, these control laws are difficult to apply in practice due to the lack of available sensors on one hand and the need of wastewater storage on the other hand (Hess and Bernard (2008)). These inconveniences can be avoided and the technological goal of the anaerobic digestion system can be achieved if the operation of the process uses the insight gained from a thorough analysis of system dynamics.

As it is generally the case for biochemical processes, the anaerobic digestion system is characterized by steady state multiplicity, i.e. several equilibria occur in the system's state space for a given set of input values. In this case, not only the input values determine the time evolution of the system but also the choice of the initial state. Hence, it is valuable to know whether or not the state of the system belongs to the set of states which determine the convergence to the desired equilibrium point.

This paper presents the estimation and visualization of stability boundaries in state space for an anaerobic digestion system with six equilibrium points. The estimation procedure consists in properly defining a set of initial states from which the system's equations are integrated in reverse time. The visualization technique consists in intersecting the estimated boundary with well selected hyperplanes. Beside simplicity and accuracy, these algorithms offer two-dimensional diagrams, which allow the operator to select appropriate initial states.

The paper is organized as follows. In Section 2 the system description is provided and its behaviour is analysed. Section 3 introduces several concepts and results from systems theory that lead to the geometric characterization of the stability boundary. The estimation and visualization algorithms are introduced in Section 4 and several conclusions are drawn in Section 5.

2. SYSTEM DESCRIPTION

The model of the anaerobic digestion system under study considers two reactions: acidogenesis and methanogenesis. In the sequel, a system involving two biochemical reactions will be called a rank two system (Sbarciog et al. (2006)). The biological transformations are described by the following reaction network:

$$a\xi_1 \rightarrow c\xi_2 + \xi_3$$
$$d\xi_2 \rightarrow CH_4 + \xi_4$$

In the first reaction, the acidogenic bacteria ξ_3 consume the organic substrate ξ_1 and produce volatile fatty acids ξ_2. In the second reaction, the methanogenic bacteria ξ_4 use the volatile fatty acids as substrate for growth and produce methane. The anaerobic digestion process must be operated such that the acidification (accumulation of volatile fatty acids) of the reactor is avoided. Thus a balance between the acidogenesis and methanogenesis must be maintained.

It is assumed that the process takes place in an ideal continuous stirred tank reactor, where the system dynamics are described by the following differential equations:

$$\dot{\xi}_1 = D(\xi_{in_1} - \xi_1) - ar_1(\xi) \quad (1)$$
$$\dot{\xi}_2 = D(\xi_{in_2} - \xi_2) + cr_1(\xi) - dr_2(\xi) \quad (2)$$
$$\dot{\xi}_3 = -D\xi_3 + r_1(\xi) \quad (3)$$
$$\dot{\xi}_4 = -D\xi_4 + r_2(\xi) \quad (4)$$

D represents the dilution rate and ξ_{in_1}, ξ_{in_2} respectively represent the concentrations of organic substrate and of volatile fatty acids in the influent. $a, c, d > 0$ are the stoichiometric coefficients. $\xi = [\,\xi_1 \quad \xi_2 \quad \xi_3 \quad \xi_4\,]' \in \mathbb{R}^{+^4}$ denotes the state vector. The reaction rates $r_1(\xi)$, $r_2(\xi)$ read:

$$r_1(\xi) = f_1(\xi_1)\xi_3 \quad (5)$$
$$r_2(\xi) = f_2(\xi_2)\xi_4 \quad (6)$$

where the growth functions are respectively of the Monod type and of the Haldane type:

$$f_1(\xi_1) = \mu_{m_1}\frac{\xi_1}{K_{s_1} + \xi_1} \quad (7)$$
$$f_2(\xi_2) = \mu_{m_2}\frac{\xi_2}{K_{s_2} + \xi_2 + \frac{\xi_2^2}{K_{i_2}}} \quad (8)$$

Table 1 gives the numerical values/ranges for the anaerobic digestion model parameters and input variables, applied in this study. These values are the same as those used in Bernard et al. (2001).

By considering a partition of the state vector of the form $\xi = [\,\xi_a \quad \xi_b\,]'$, where $\xi_a = [\,\xi_3 \quad \xi_4\,]'$ and $\xi_b = [\,\xi_1 \quad \xi_2\,]'$, and a linear transformation of the states $x_a = \xi_a$, $x_b = \xi_b - C_bC_a^{-1}\xi_a$, a canonical state space representation of the anaerobic digestion system can be obtained (Bastin and Dochain (1990); Bastin and Van Impe (1995)):

Table 1. Numerical values/ranges of the anaerobic digestion model parameters and input variables

a	42.14		K_{s_1}	7.1	g/l
c	116.5	mmole/g	K_{s_2}	9.28	mmole/l
d	268	mmole/g	K_{i_2}	256	mmole/l
μ_{m_1}	1.2	day^{-1}	ξ_{in_1}	$[\,0 \;\; 50\,]$	g/l
μ_{m_2}	0.74	day^{-1}	ξ_{in_2}	$[\,0 \;\; 200\,]$	mmole/l
			D	$[\,0 \;\; 1.5\,]$	day^{-1}

$$\dot{x}_a = D(w_a - x_a) + C_a\rho(x) \quad (9)$$
$$\dot{x}_b = D(w_b - x_b) \quad (10)$$

with

$$x_a \triangleq \begin{bmatrix} x_3 \\ x_4 \end{bmatrix} \in \mathbb{R}^{+^2};\; x_b \triangleq \begin{bmatrix} x_1 \\ x_2 \end{bmatrix} \in \mathbb{R}^2;\; C_a = I_2;$$
$$C_b = \begin{bmatrix} -a & 0 \\ c & -d \end{bmatrix};\; \rho(x) \triangleq \begin{bmatrix} \rho_1(x) \\ \rho_2(x) \end{bmatrix} \in \mathbb{R}^{+^2};$$
$$w_a = \begin{bmatrix} w_3 \\ w_4 \end{bmatrix} \triangleq \begin{bmatrix} 0 \\ 0 \end{bmatrix};\; w_b = \begin{bmatrix} w_1 \\ w_2 \end{bmatrix} \triangleq \begin{bmatrix} \xi_{in_1} \\ \xi_{in_2} \end{bmatrix} \in \mathbb{R}^{+^2}$$

$$\rho_i(x) = r_i(\xi)|_{\xi_a = x_a;\; \xi_b = x_b + C_bC_a^{-1}x_a},\; i = 1, 2$$

The canonical model consists of a nonlinear part of dimension 2 dynamically coupled with a linear part of dimension 2. It presents a reduction in the order of the nonlinear dynamics, which makes the system analysis easier. This model has been used to analyse in detail the behaviour of the anaerobic digestion system (see Sbarciog (2008)) and will be subsequently employed in illustrating the stability boundary estimation procedure.

Several properties can be stated for the system (9), (10) (see Sbarciog (2008)):

- All system's trajectories are bounded.
- The physical state space of the model in canonical state variables is given by:

  $S_x = \{x \in \mathbb{R}^4;\; \xi_1 = x_1 - ax_3 \geq 0;$
  $\xi_2 = x_2 + cx_3 - dx_4 \geq 0;\; \xi_3 = x_3 \geq 0;\; \xi_4 = x_4 \geq 0\}$
- Every system's trajectory $x(t)$ that starts at time $t = 0$ in an initial state $x_0 = x(0) \in S_x$ stays in S_x for all $t \geq 0$. $x(t)$ is bounded for $t \geq 0$ and converges to $\Delta = \{x \in S_x;\; x_1 = w_1,\; x_2 = w_2\}$
- All the equilibrium points lie in Δ. There are no nontrivial closed trajectories and each trajectory converges to an equilibrium point as $t \rightarrow +\infty$.
- On Δ the model behaves as an autonomous second order system described by (9) where $x_1 = w_1$, $x_2 = w_2$.
- There are no equilibrium points for which $\xi_1 = w_1 - ax_3 = 0$ or for which $\xi_2 = w_2 + cx_3 - dx_4 = 0$.
- A system trajectory which starts on the x_3-axis stays on the x_3-axis as time increases. A system trajectory which starts on the x_4-axis stays on the x_4-axis as time increases.

Depending on the magnitude of the dilution rate D and of the component concentrations in the inflow ξ_{in_1}, ξ_{in_2}, the system may possess up to six equilibria. The determination of the regions in the input spaces for which various numbers of equilibria occur has been presented

Table 2. The analytical expressions of the system's equilibria

Canonical states	Physical states
$\hat{x}_A = \begin{bmatrix} w_1 \\ w_2 \\ 0 \\ 0 \end{bmatrix}$	$\hat{\xi}_A = \begin{bmatrix} \xi_{in_1} \\ \xi_{in_2} \\ 0 \\ 0 \end{bmatrix}$
$\hat{x}_B = \begin{bmatrix} w_1 \\ w_2 \\ \frac{1}{a}(w_1 - \hat{\xi}_{B_1}) \\ 0 \end{bmatrix}$	$\hat{\xi}_B = \begin{bmatrix} \hat{\xi}_{B_1} \\ \xi_{in_2} + \frac{c}{a}(\xi_{in_1} - \hat{\xi}_{B_1}) \\ \frac{1}{a}(\xi_{in_1} - \hat{\xi}_{B_1}) \\ 0 \end{bmatrix}$
$\hat{x}_M = \begin{bmatrix} w_1 \\ w_2 \\ 0 \\ \frac{1}{d}(w_2 - \hat{\xi}_{M_2}) \end{bmatrix}$	$\hat{\xi}_M = \begin{bmatrix} \xi_{in_1} \\ \hat{\xi}_{M_2} \\ 0 \\ \frac{1}{d}(\xi_{in_2} - \hat{\xi}_{M_2}) \end{bmatrix}$; $M = C, D$
$\hat{x}_N = \begin{bmatrix} w_1 \\ w_2 \\ \frac{1}{a}(w_1 - \hat{\xi}_{N_1}) \\ \hat{x}_{N_4} \end{bmatrix}$	$\hat{\xi}_N = \begin{bmatrix} \hat{\xi}_{N_1} \\ \hat{\xi}_{N_2} \\ \frac{1}{a}(\xi_{in_1} - \hat{\xi}_{N_1}) \\ \hat{\xi}_{N_4} \end{bmatrix}$; $N = E, F$
$\hat{x}_{N_4} = \frac{1}{d}\left[w_2 - \hat{\xi}_{N_2} + \frac{c}{a}(w_1 - \hat{\xi}_{N_1})\right]$	
$\hat{\xi}_{N_4} = \frac{1}{d}\left[\xi_{in_2} - \hat{\xi}_{N_2} + \frac{c}{a}(\xi_{in_1} - \hat{\xi}_{N_1})\right]$	

in Sbarciog (2008). Here, the input values have been fixed to $D = 0.45\text{day}^{-1}$, $\xi_{in_1} = 40\text{g/l}$, $\xi_{in_2} = 175\text{mmole/l}$ such that the most complex case is obtained in order to emphasize the efficiency of the estimation and visualization algorithms.

The equilibrium points are the solutions of

$$x_1 = w_1 = \xi_{in_1} \tag{11}$$
$$x_2 = w_2 = \xi_{in_2} \tag{12}$$
$$[-D + f_1(\xi_1)]\, x_3 = 0 \tag{13}$$
$$[-D + f_2(\xi_2)]\, x_4 = 0 \tag{14}$$

where $\xi_1 = w_1 - ax_3$, $\xi_2 = w_2 + cx_3 - dx_4$.

Table 2 lists the analytical expressions of the equilibrium points. Note that the subscript M is used to refer to two equilibria, $\hat{x}_C$ ($\hat{\xi}_C$) and $\hat{x}_D$ ($\hat{\xi}_D$). Similarly, the subscript N is used to refer to the equilibrium points $\hat{x}_E$ ($\hat{\xi}_E$) and $\hat{x}_F$ ($\hat{\xi}_F$). $\hat{\xi}_{B_1} = \hat{\xi}_{N_1}$ is the unique solution of

$$f_1(\xi_1) = D \tag{15}$$

$\hat{\xi}_{M_2} = \hat{\xi}_{N_2} = \hat{\xi}_{C_2}, \hat{\xi}_{D_2}$, with $\hat{\xi}_{C_2} < \hat{\xi}_{D_2}$ are the two solutions of

$$f_2(\xi_2) = D \tag{16}$$

The technical relevance of the equilibria is straightforward: $\hat{x}_A$ represents the total wash out state of the system, in which no conversion is realized; $\hat{x}_B$ corresponds to the wash out of the methanogenic bacteria, which prevents the conversion to methane and favors the accumulation of the volatile fatty acids ξ_2; $\hat{x}_M$ correspond to the wash out of the acidogenic bacteria, no conversion of the organic substrate is realized; in $\hat{x}_N$ both substrates are consumed.

The local stability of the equilibrium points is assessed via the linearization principle. The Jacobian matrix of the system dynamics on the set Δ reads:

$$J(x) = \begin{bmatrix} J_1 & 0 \\ J_2 & J_3 \end{bmatrix} \tag{17}$$

with

$$J_1 = -D + f_1(\xi_1) + f_{1_d}(\xi_1)x_3(-a)$$
$$J_2 = f_{2_d}(\xi_2)x_4 c$$
$$J_3 = -D + f_2(\xi_2) + f_{2_d}(\xi_2)x_4(-d)$$

where $f_{i_d}(\xi_j) = \dfrac{\partial f_i(\xi_j)}{\partial \xi_j}$, $i, j = 1, 2$. There are two eigenvalues corresponding to the nonlinear part

$$\lambda_1 = -D + f_1(\xi_1) + f_{1_d}(\xi_1)x_3(-a) \tag{18}$$
$$\lambda_2 = -D + f_2(\xi_2) + f_{2_d}(\xi_2)x_4(-d) \tag{19}$$

and two equal eigenvalues corresponding to the linear part

$$\lambda_3 = \lambda_4 = -D \tag{20}$$

An equilibrium point is *hyperbolic* if the eigenvalues do not lie on the imaginary axis. The equilibrium point is locally asymptotically stable (l.a.s.) if all eigenvalues have negative real parts. Otherwise, it is unstable and has an *index*, which equals the number of eigenvalues with positive real parts.

Evaluating the eigenvalues of the Jacobian matrix for each of the six equilibrium points of the system, it can be concluded that $\hat{x}_A$, $\hat{x}_C$ and $\hat{x}_F$ are unstable with index 1, $\hat{x}_D$ is unstable with index 2, while $\hat{x}_B$ and $\hat{x}_E$ are l.a.s. All equilibria are hyperbolic.

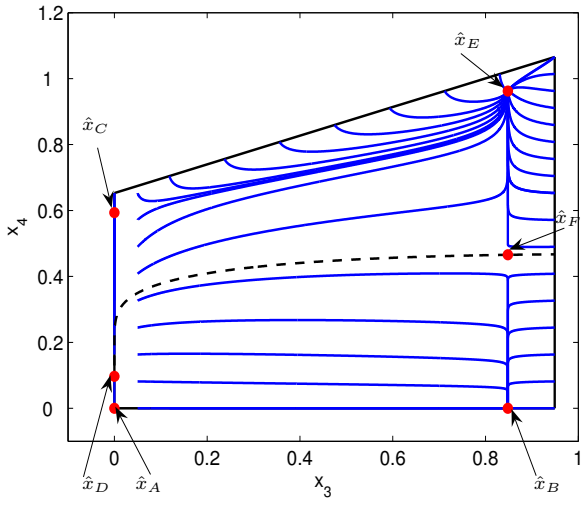

Fig. 1. The phase portrait of the system on the Δ-plane

Fig. 1 presents the phase portrait of the system on the Δ-plane. Trajectories on the x_4-axis either converge to $\hat{x}_A$ or $\hat{x}_C$ depending on whether $x_4(0) < \hat{x}_{D_4}$ or $x_4(0) > \hat{x}_{D_4}$. Trajectories on the x_3-axis converge to $\hat{x}_B$. If $x_3(0) > 0$ and $x_4(0) > 0$, then the system will be led to either $\hat{x}_B$ or $\hat{x}_E$ depending on whether the initial state is lying below or above the stability boundary $\partial\Omega(\hat{x}_E) = \partial\Omega(\hat{x}_B)$. Since $\hat{x}_B$ represents the acidification point of the system, the convergence to this equilibrium point should be prevented. The initial state of the system x_0 should be carefully

chosen such that $x_0 \in \Omega(\hat{x}_E)$ (the region of attraction of $\hat{x}_E$), where

$$\Omega(\hat{x}_E) \triangleq \{x_0 \in S_x;\ x(t,x_0) \to \hat{x}_E,\ \text{for}\ t \to +\infty\}$$

It is of outmost importance to accurately estimate the stability boundary $\partial\Omega(\hat{x}_E)$ (dashed line in Fig. 1), which separates the regions of attraction $\Omega(\hat{x}_B)$ and $\Omega(\hat{x}_E)$.

3. THEORETICAL CONCEPTS AND RESULTS

To describe the procedure for estimating the stability boundary $\partial\Omega(\hat{x}_E)$, the following concepts are needed:

The *stable manifold* of a hyperbolic equilibrium point $\hat{x}_i$ is defined as

$$W^s(\hat{x}_i) \triangleq \{x_0 \in \mathbb{R}^n;\ x(t,x_0) \to \hat{x}_i,\ \text{for}\ t \to +\infty\}$$

while the *unstable manifold* of a hyperbolic equilibrium point $\hat{x}_i$ is given by

$$W^u(\hat{x}_i) \triangleq \{x_0 \in \mathbb{R}^n;\ x(t,x_0) \to \hat{x}_i,\ \text{for}\ t \to -\infty\}$$

If all equilibria are hyperbolic, the system has no closed trajectories, all trajectories on the stability boundary are bounded and the transversality condition (see Chiang et al. (1988)) is satisfied, then the following two theorems stated by Chiang et al. (1988) can be used to characterize the stability boundary:

Theorem 1.

$$\hat{x}_j \in \partial\Omega(\hat{x}_i)\ \text{ if and only if }\ W^u(\hat{x}_j) \cap \Omega(\hat{x}_i) \neq \emptyset \tag{21}$$

Theorem 2.

$$\partial\Omega(\hat{x}_i) = \bigcup_{\hat{x}_j \in \partial\Omega(\hat{x}_i)} W^s(\hat{x}_j) \tag{22}$$

According to (22), the stability boundary $\partial\Omega(\hat{x}_i)$ consists of the union of stable manifolds of all equilibria lying on $\partial\Omega(\hat{x}_i)$. This condition can be checked using (21).

Additionally, if there are no interior boundary sets (i.e. the stability region is the interior of its closure)

$$\Omega(\hat{x}_i) = int\ \bar{\Omega}(\hat{x}_i) \tag{23}$$

then Zaborszky et al. (1988) prove that

Theorem 3.

$$\partial\Omega(\hat{x}_i) = \bigcup_{\hat{x}_k \in \Psi} \overline{W}^s(\hat{x}_k) \tag{24}$$

where

$$\Psi \triangleq \{\hat{x}_k\,;\ index\ \hat{x}_k = 1\,;\ \hat{x}_k \in \partial\Omega(\hat{x}_i)\} \tag{25}$$

Hence the stability boundary $\partial\Omega(\hat{x}_i)$ is the union of the closures of stable manifolds of all index 1 equilibria lying on $\partial\Omega(\hat{x}_i)$.

4. ESTIMATION AND VISUALIZATION OF THE STABILITY BOUNDARY

In the physical state space of the anaerobic digestion system, the only index 1 equilibrium point lying on the stability boundary $\partial\Omega(\hat{x}_E)$ is $\hat{x}_F$. This can be easily checked using Theorem 1: The unique positive eigenvalue of $J(\hat{x}_F)$ and the corresponding eigenvector e_1 are determined. For a sufficiently small $|\varepsilon e_1|$ either $x_{01} = \hat{x}_F - \varepsilon e_1 \in \Omega(\hat{x}_E)$ or $x_{02} = \hat{x}_k + \varepsilon e_1 \in \Omega(\hat{x}_E)$. Integrating numerically the system equations from these initial conditions leads to the conclusion that $x_{01} \in \Omega(\hat{x}_E)$ and $x_{02} \in \Omega(\hat{x}_B)$.

Next, an estimate of $W^s(\hat{x}_F)$ must be computed such that $W^s(\hat{x}_F)_{est} \subset \Omega(\hat{x}_E)$ and $W^s(\hat{x}_F)_{est} \to W^s(\hat{x}_F)$ as some algorithmic parameter $\varepsilon \to 0$. In this way an estimated stability boundary can be obtained, in principle of any desired accuracy, lying inside $\Omega(\hat{x}_E)$. This estimate $\partial\Omega(\hat{x}_E)_{est}$ surrounds an estimated stability region $\Omega(\hat{x}_E)_{est} \subset \Omega(\hat{x}_E)$. To solve this problem a trajectory reversing algorithm (see Loccufier and Noldus (2000)) can be applied: The system's state equations (9), (10) are integrated in reverse time, starting from initial states on a suitably constructed anchor set γ inside $\Omega(\hat{x}_E)$ and close to $\hat{x}_F$. γ can be chosen as the boundary of a sufficiently small 3-dimensional disk surrounding x_{01} and lying in a hyperplane parallel to $T_{\hat{x}_F}[W^s(\hat{x}_F)]$, the tangent space to $W^s(\hat{x}_F)$ at the equilibrium point $\hat{x}_F$.

The anchor set is given by

$$\gamma \triangleq \left\{x \in S_x;\ b'(x - x_{01}) = 0,\ a_0^2(x - x_{01})'(x - x_{01}) = \varepsilon^2\right\} \tag{26}$$

where $b \in \mathbb{R}^4$ is orthogonal with the 3 eigenvectors of $J(\hat{x}_F)$ corresponding to its stable eigenvalues.

Since $x_{01} \in \Omega(\hat{x}_E)$ and $\Omega(\hat{x}_E)$ is an open set, the condition

$$\gamma \subset \Omega(\hat{x}_E) \tag{27}$$

is fulfilled if $\varepsilon > 0$ is chosen sufficiently small and $a_0 > 0$ sufficiently large. The condition (27) must be verified by simulation.

The solutions in reverse time of (9), (10), where the initial states $x_0 \in \gamma$, and the cone segment connecting γ with $\hat{x}_F$ define the manifold $W^s(\hat{x}_F)_{est}$.

The estimated stability boundary is a 3-dimensional surface. To visualize the extent of the region of attraction of $\hat{x}_E$ in state space, a simple technique consists in computing intersections of $\partial\Omega(\hat{x}_E)_{est}$ with well selected hyperplanes. Thus intersections in the x_a-plane can be obtained by intersecting the boundary with sets $H = \{x \in S_x;\ x_b = \eta\}$ for constant vectors $\eta = \begin{bmatrix}\eta_1 \\ \eta_2\end{bmatrix}$.

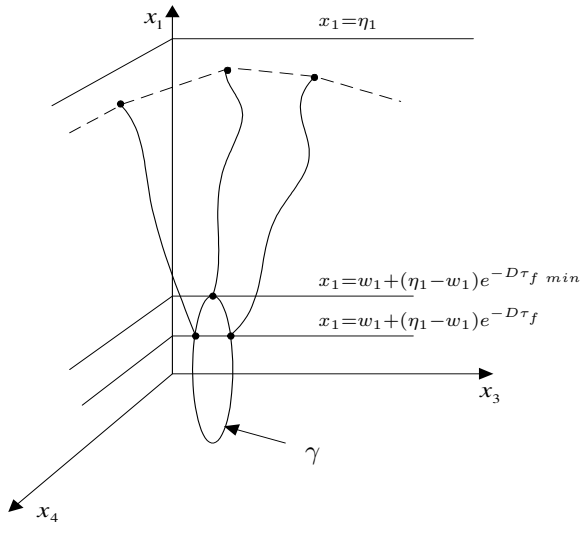

Fig. 2. Obtaining intersections on the x_a-plane

Suppose a trajectory of (9), (10), computed in reverse time $\tau = -t$ and starting at $\tau = 0$ in a point of γ, reaches the set H at time $\tau = \tau_f$. Then

$$x_b(\tau) = w_b + (x_b(0) - w_b)e^{D\tau} \tag{28}$$

$$x_b(0) = w_b + (\eta - w_b)e^{-D\tau_f} \tag{29}$$

The intersection is found by solving

$$\frac{dx_a}{d\tau} = -(D(w_a - x_a) + C_a\rho(x)) \tag{30}$$

where $x_b(\tau) = w_b + (\eta - w_b)e^{D(\tau-\tau_f)}$ for initial values $x_a(0)$ on the set:

$$\gamma_0 \triangleq \gamma \cap \left\{x_b = w_b + (\eta - w_b)e^{-D\tau_f}\right\} \tag{31}$$

There exists a time $\tau_{f\ min}$ such that γ_0 contains exactly two points for $\tau_f > \tau_{f\ min}$ and γ_0 is empty for $\tau_f < \tau_{f\ min}$. The points $x_a(\tau_f)$, $\tau_{f\ min} < \tau_f < +\infty$, yield the desired intersection curve. Fig 2 presents intuitively the procedure in the $x_3 - x_4 - x_1$-space.

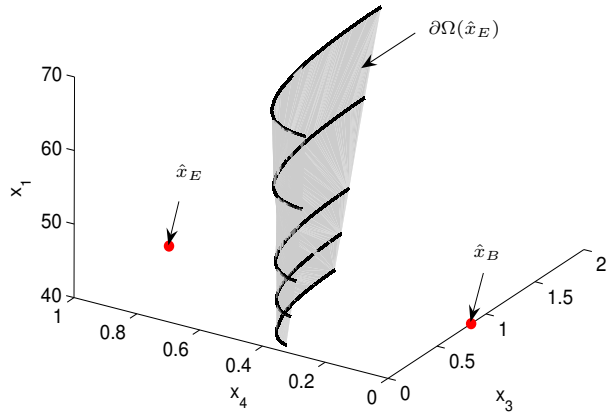

Fig. 3. The estimated stability boundary intersected with

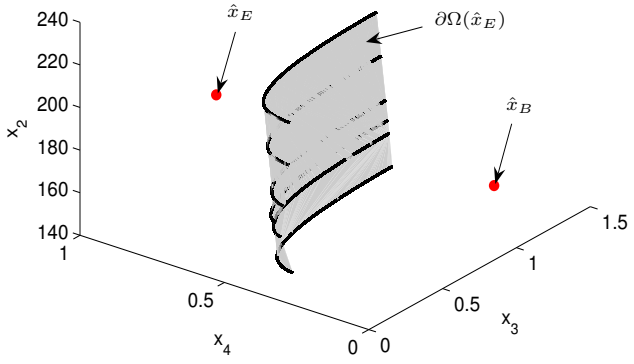

Fig. 4. The estimated stability boundary intersected with the set $x_1 = w_1 + 5$

Fig. 3 illustrates the estimated stability boundary intersected with the set $x_2 = w_2 + 5$ and $41 \leq x_1 \leq 70$, while Fig. 4 illustrates the estimated stability boundary intersected with the set $x_1 = w_1 + 5$ and $170 \leq x_2 \leq 225$. Initial states lying on the left hand side of the boundary will lead the system to the operating point $\hat{x}_E$, those lying on the right hand side of $\partial\Omega(\hat{x}_E)$ will lead the system to the acidification point $\hat{x}_B$. It is obvious that due to the inhibition effects the extent of the stability boundary in the state space is changing. An operator can see more clearly these effects on the 2-dimensional plots of Figs. 5, 6 and 7.

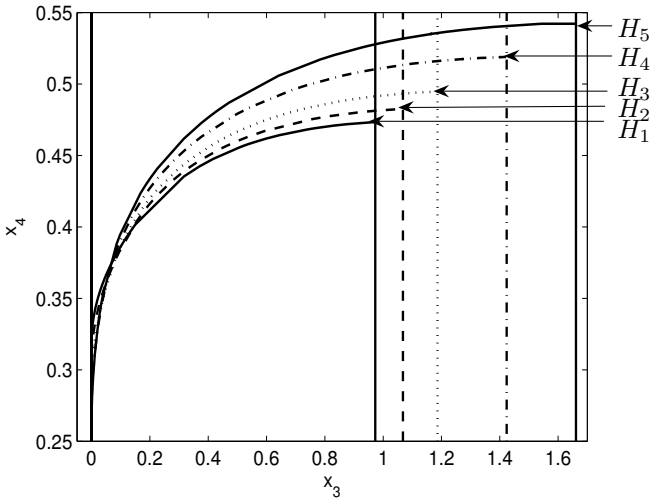

Fig. 5. Intersection curves in the x_a-plane of $\partial\Omega(\hat{x}_E)$ with planes of constant x_2

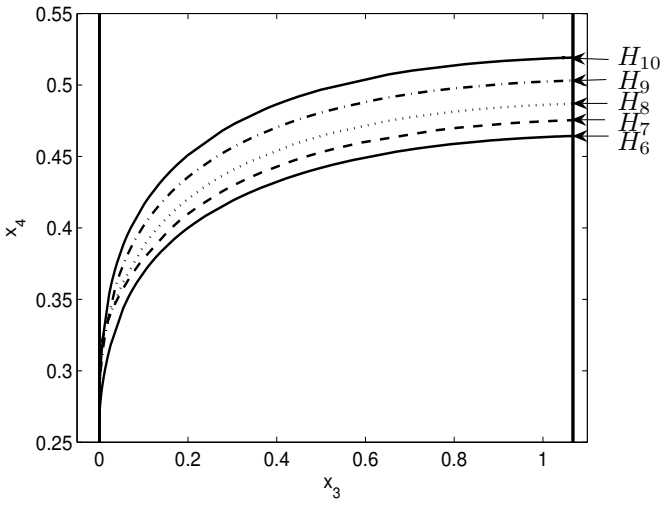

Fig. 6. Intersection curves in the x_a-plane of $\partial\Omega(\hat{x}_E)$ with planes of constant x_1

Fig. 5 presents intersections of the estimated stability boundary with the planes $H_i = \{x_1 = w_1 + \alpha_i, x_2 = \eta_2 = w_2 + 5\}$, $i = 1, \ldots, 5$, where $\alpha_i \in \{1, 5, 10, 20, 30\}$. The vertical line on the left hand side of the intersection curves represents the physical boundary $\xi_3 = 0$, the vertical lines on the right hand side represent the physical boundary $\xi_1 = x_1 - ax_3 = 0$ on the plane H_i. x_1 has a different value on each of the planes H_i, which implies also a different value for x_3. This makes the boundary to shift

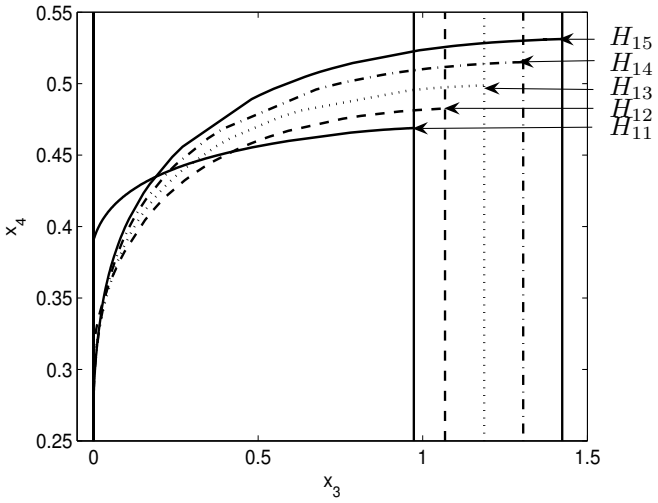

Fig. 7. Intersection curves in the x_a-plane of $\partial\Omega(\hat{x}_E)$ with planes parallel to Δ

to the right hand side for increasing values of x_1. Any initial state of the system on the plane H_i lying above the corresponding intersection curve and within the physical boundaries will determine the convergence of the anaerobic digestion process to the operating point $\hat{x}_E$. A higher value of x_1 implies a decrease of the size of $\Omega(\hat{x}_E)$.

Fig. 6 shows the intersections of the estimated stability boundary with planes $H_i = \{x_1 = \eta_1 = w_1 + 5, x_2 = w_2 + \beta_i\}$, $i = 6, \ldots, 10$, where $\beta_i \in \{-5, 1, 10, 30, 50\}$. The vertical line on the left hand side of the intersection curves represents the physical boundary $\xi_3 = 0$, the vertical line on the right hand side represents the physical boundary $\xi_1 = 0$ on the plane H_i. Any initial state of the system on the plane H_i lying above the corresponding intersection curve and within the physical boundaries will determine the convergence of the anaerobic digestion process to the operating point $\hat{x}_E$. A higher value of x_2 determines also a decrease of the size of $\Omega(\hat{x}_E)$.

The estimated stability boundary has been intersected also with planes parallel to Δ and the results are displayed in Fig. 7. These planes have the form $H_i = \{x_1 = \eta_1 = w_1 + \delta_i, x_2 = w_2 + \delta_i\}$, $i = 11, \ldots, 15$, where $\delta_i \in \{1, 5, 10, 15, 20\}$.

5. CONCLUSIONS

An anaerobic digestion system with two biochemical reactions has been presented in this paper. The set of equilibrium points of this system is globally convergent. For the selected input values, six equilibrium points occur in the system state space. Two of them, $\hat{x}_B$ and $\hat{x}_E$, are locally asymptotically stable and the system dynamics will settle down in one or the other, depending on the initial conditions. $\hat{x}_B$ is the acidification point, which should be avoided during operation.

The two sets of initial conditions from where the operation ends up in either $\hat{x}_B$ or $\hat{x}_E$ are separated by the system stability boundary $\partial\Omega(\hat{x}_E)$. The geometric characterization of the stability boundary has been described and a methodology for estimating this boundary has been introduced. The algorithm allows to find an estimate of any desired accuracy. Although it mainly involves the integration in reverse time of system's equations, of a great importance is the choice of the initial states. Exploiting the system's properties, a mathematical expression of the anchor set has been given.

The estimated stability boundary is a surface in a high dimensional space. To make use of it in properly operating the system, a visualization technique has been introduced. It consists of intersecting the estimated stability boundary with well selected sets allowing thus to visualize the extent of the stability region in a three-dimensional or even two-dimensional space. Hence, intersection curves are obtained, which can be easily interpreted by the system's operator.

REFERENCES

Alcaraz-González, V., Salazar-Peña, R., González-Álvarez, V., Gouzé, J.L., and Steyer, J.P. (2005). A tunable multivariable nonlinear robust observer for biological systems. *Comptes Rendus Biologies*, 328, 317–325.

Bastin, G. and Dochain, D. (1990). *On-line estimation and adaptive control of bioreactors*. Elsevier, Amsterdam.

Bastin, G. and Van Impe, J.F. (1995). Nonlinear and adaptive control in biotechnology: a tutorial. *European Journal of Control*, 1, 37–53.

Bernard, O., Hadj-Sadok, Z., Dochain, D., Genovesi, A., and Steyer, J.P. (2001). Dynamical model development and parameter identification for an anaerobic wastewater treatment process. *Biotechnology and Bioengineering*, 75, 424–438.

Chiang, H.D., Hirsch, M.W., and Wu, F.F. (1988). Stability regions of nonlinear autonomous dynamical systems. *I.E.E.E. Trans. on Automatic Control*, 33, 16–27.

Hess, J. and Bernard, O. (2008). Design and study of a risk management criterion for an unstable anaerobic wastewater treatment process. *Journal of Process Control*, 18, 71–79.

Loccufier, M. and Noldus, E. (2000). A new trajectory reversing method for estimating stability regions of autonomous nonlinear systems. *Nonlinear Dynamics*, 21, 265–288.

Mailleret, L., Bernard, O., and Steyer, J.P. (2003). Robust regulation of anaerobic digestion processes. *Water Science & Technology*, 48, 87–94.

Mailleret, L., Bernard, O., and Steyer, J.P. (2004). Nonlinear adaptive control for bioreactors with unknown kinetics. *Automatica*, 40, 1379–1385.

Perrier, M. and Dochain, D. (1993). Evaluation of control strategies for anaerobic digestion processes. *International Journal of Adaptive Control and Signal Processing*, 7, 309–321.

Sbarciog, M. (2008). *The stability of biochemical reaction systems*. PhD thesis, Ghent University.

Sbarciog, M., Loccufier, M., and Noldus, E. (2006). Anticipating operational and wash-out conditions in biotechnological reactors. *American Institute of Physics Conference Proceedings*, 839, 618–629.

Zaborszky, J., Huang, G., Zheng, B., and Leung, T.C. (1988). On the phase portrait of a class of large nonlinear dynamic systems such as the power system. *IEEE Trans. on Automatic Control*, 33, 4–15.